Single cell neurophysiology project

Jaume Colom
jaume.colom@estudiantat.upc.edu

November 2, 2020

The Morris-Lecar model

The Morris–Lecar model is a biological neuron model developed by Catherine Morris and Harold Lecar to reproduce the variety of oscillatory behavior in relation to Ca++ and K+ conductance in the muscle fiber of the giant barnacle [1].

Figure 1: Photography of a giant barnacle. Source: [2]

The Morris-Lecar model of an excitable system is a two-dimensional system of nonlinear differential equations. It is a simplification of the Hodgkin-Huxley [3] model of spike generation in squid giant axons.

Qualitatively, this system of equations describes the complex relationship between membrane potential and the activation of ion channels within the membrane: the potential depends on the activity of the ion channels, and the activity of the ion channels depends on the voltage. As parameters are altered different classes of neuron behavior are exhibited. τ_W is associated with the relative time scales of the firing dynamics, which varies broadly from cell to cell and exhibits significant temperature dependency.

The system is described by the following differential equations:

$$\frac{dV}{dt} = \frac{1}{C_M}(\bar{g}_L(V - V_L) + \bar{g}_{Ca}M_\infty(V)(V - V_{Ca}) + \bar{g}_K w\,(V - V_K) + I_{\text{app}})$$

$$\frac{dW}{dt} = \phi\,(W_\infty(V) - W)\frac{1}{\tau_W(V)}$$

Where:

$$M_\infty(V) = 0.5 * (1 + \tanh((V - V_1)/V_2))$$
$$W_\infty(V) = 0.5 * (1 + \tanh((V - V_3)/V_4))$$
$$\tau_W(V) = 1/(cosh((V - V_3)/(2 \cdot V_4)))$$

Here I_{app} is a stimulus current ($\mu A/cm^2$). The constants $\bar{g}_L, \bar{g}_{Ca}\bar{g}_K$ denote the maximum conductances ($mmho/cm^2$) of leak currents, Ca^{2+} and K^+; And V_L, V_{Ca}, V_K (mV) represent the

equilibrium potentials of corresponding ionic currents. V_1,V_2,V_3 and V_4 (mV) are model parameters.

Bifurcation diagram and stability analysis

The bifurcation diagram of a dynamical system shows the values visited or approached asymptotically (fixed points, periodic orbits or chaotic attractors) of a system as a function of a bifurcation parameter in the system.

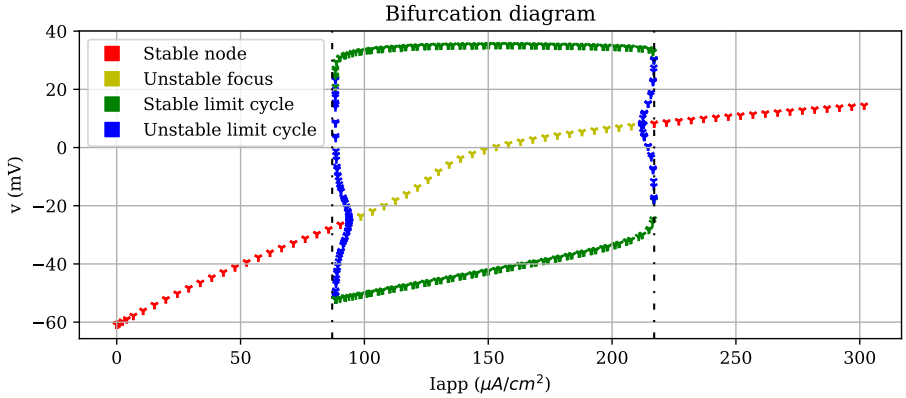

Figure 1: Bifurcation diagram of the Morris-Lecar model

In Figure 1 we see the bifurcation diagram of the Morris Lecar model. There are three different sections, the first corresponds to $I_{app} \in (0, 87)$ with subtrehsold activity, the second to $I_{app} \in (87, 212)$ with spiking activity, and the last $I_{app} \in (212, \infty)$ with bistability.

Let's analyze the system for three different I_{app} values, $I_{app} \in (0, 160, 300)$. In Figure 2 we see a temporal simulation of the model in the three scenarios, each with three different V starting points, equilibrium, equilibrium + 25 and equilibrium + 50, to see the effect of a perturbation in the system.

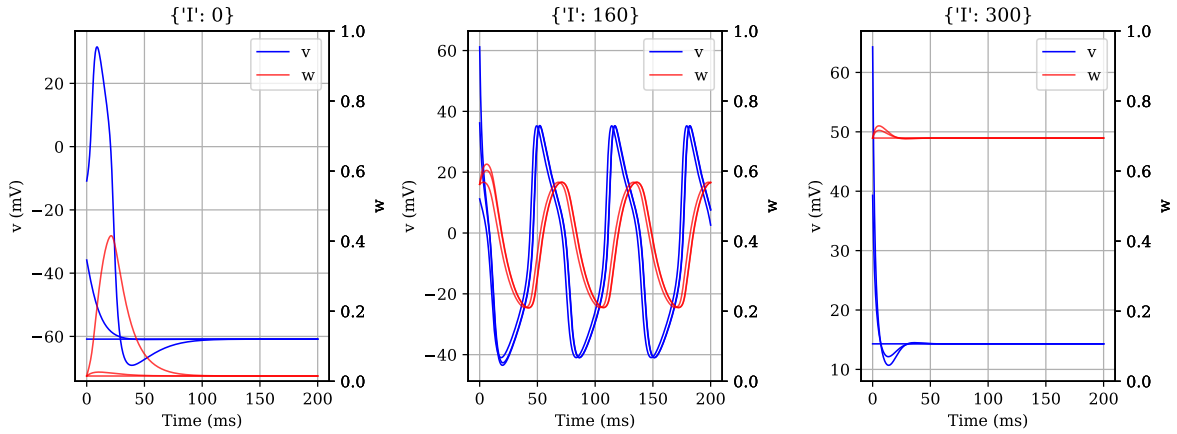

Figure 2: Temporal simulation with three scenarios and three starting points

In the first scenario we observe how a big enough perturbation kicks the system out of stability, creates a voltage spike and cames back to equilibria point, but if the perturbation is not big enough the system doesn't. In the second scenario, the perturbation does not affect the behaviour of the system, after a short transitory phase the system comes to the periodic oscillation. In the final scenario the perturbations don't affect the system neither, it always ends up at saturation point.

We find the equilibria points when isoclines cross. Isoclines are the manifolds on which one component of the flow is null, in our case:

$$\frac{dv}{dt} = 0 \Leftrightarrow w = -\frac{\bar{g}_L(V - V_L) + \bar{g}_{Ca}M_\infty(V)(V - V_{Ca}) + \bar{g}_K w\,(V - V_K) + I_{\text{app}}}{\bar{g}_K\,(V - V_K)}$$

$$\frac{dw}{dt} = 0 \Leftrightarrow w = W_\infty(V)$$

The behaviour of the points can be classified using their eigenvalues, in this case we find the following points. In the first scenario there is one equilibrium point at $(-60.855, 0.015)$ with eigenvalues $-0.8222 + 0.0158j$ and $-0.8222 - 0.0158j$ so it is a stable focus. In the second scenario there is one equilibrium point at $(-0.4598, 0.4590)$ with eigenvalues $0.2639 + 0j$ and $0.0328 + 0j$ so it is a unstable node. And in the third scenario there is one equilibrium point at $(14.302, 0.6943)$ with eigenvalues $-0.1366 + 0.1164j$ and $-0.1366 - 0.1164j$ so it is a stable focus. The next diagram is a plot with the isoclines, the phase diagram and the equilibria points:

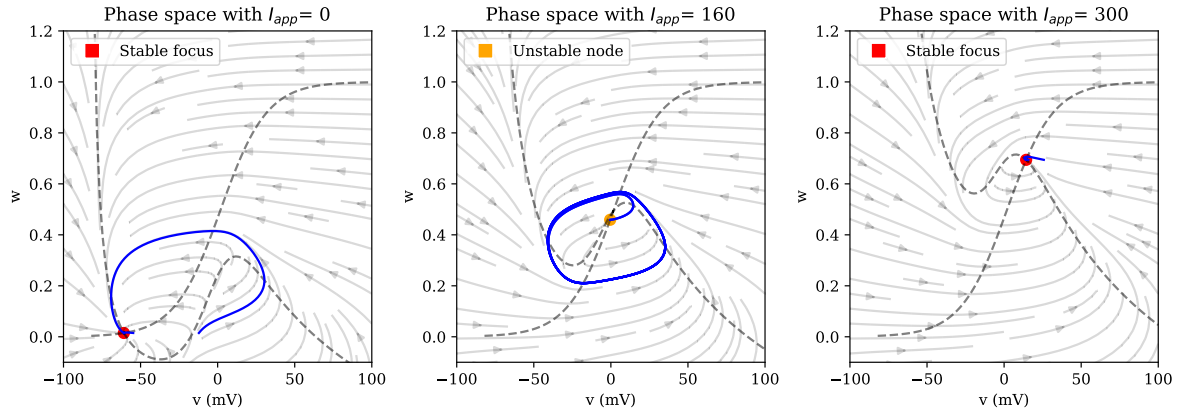

Figure 3: Phase plot with three scenarios and three initial conditions

The f-I curve and 2-parameter bifurcation

In the next plot (figure 4) we see the relationship between the Intensity (mA) and the frequency (Hz) in the oscillatory section of the model $I_{app} \in (87, 212)$. The green points correspond to the stable limit cycle and the blue points to the unstable limit cycle. They produce a smooth curve that goes from around 5Hz to 16Hz depending on the I_{app}

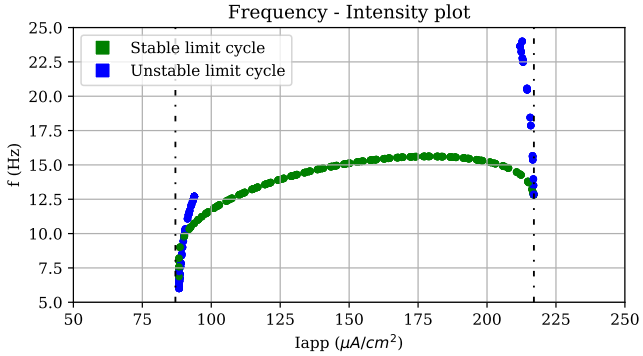

Figure 4: Frequency intensity relationship in terms of I_{app} plot

The 2-parameter bifurcation shows the Hopf bifurcations on the phase space of two variables, I_{app} and v3 in this case. In the original parameter set the v3 parameter was set at 2 mV, so we

can see in the 2-parameter bifurcation plot that the the two Hopf bifurcations appear at 87 and 217 $/cm^2$.

An interesting behaviour is that both bifurcations cross around I_{app}=50, and that the second one disappears before I_{app}=50.

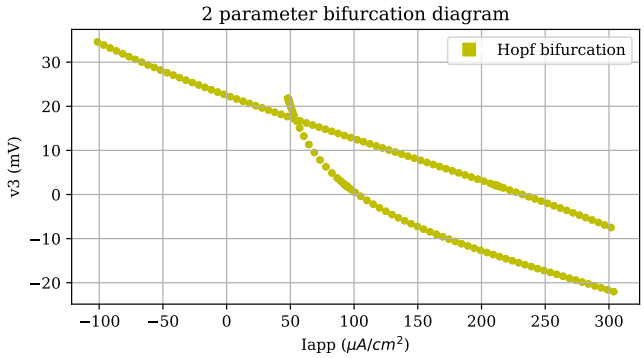

Figure 5: 2-parameter bifurcation diagram

With this information now it is interesting to study the behaviour of the system when the two Hopf bifurcations cross, this is around the 20 mV value for v3. In figure 6 we see the bifurcation diagram for v3 equals 20mv.

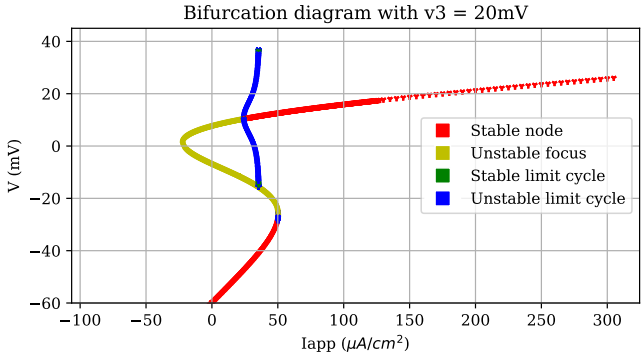

Figure 6: 2-parameter bifurcation diagram

In this scenario we get some interesting behaviour. There are two Hopf bifurcations, one very small and the second is larger at around the 50 $/cm^2$ mark. Both Hopf bifurcations begin but they vanish without closing themselves. Furthermore the second Hopf bifurcation connects to the main bifurcation, at the point around 40 $/cm^2$ and -15 mv. This produces an homoclinic bifurcation. Further studies on this bifurcation should be performed to get a thorough understanding of the system around this point.

Non-autonomous model

So far we have considered the behavior of the system under a constant stimulus I_{app}. However, it is possible to extend this model to cases where the stimulus is more complex, by making I_{app} a function of time.

$$\begin{cases} \frac{dV}{dt} = \frac{1}{C_M}(\bar{g}_L(V - V_L) + \bar{g}_{Ca}M_\infty(V)(V - V_{Ca}) + \bar{g}_K w\,(V - V_K) + I_{\text{app}}(t)) \\ \frac{dW}{dt} = \phi\,(W_\infty(V) - W)\frac{1}{\tau_W(V)} \end{cases} \tag{1}$$

Note that now the system is **non-autonomous**.

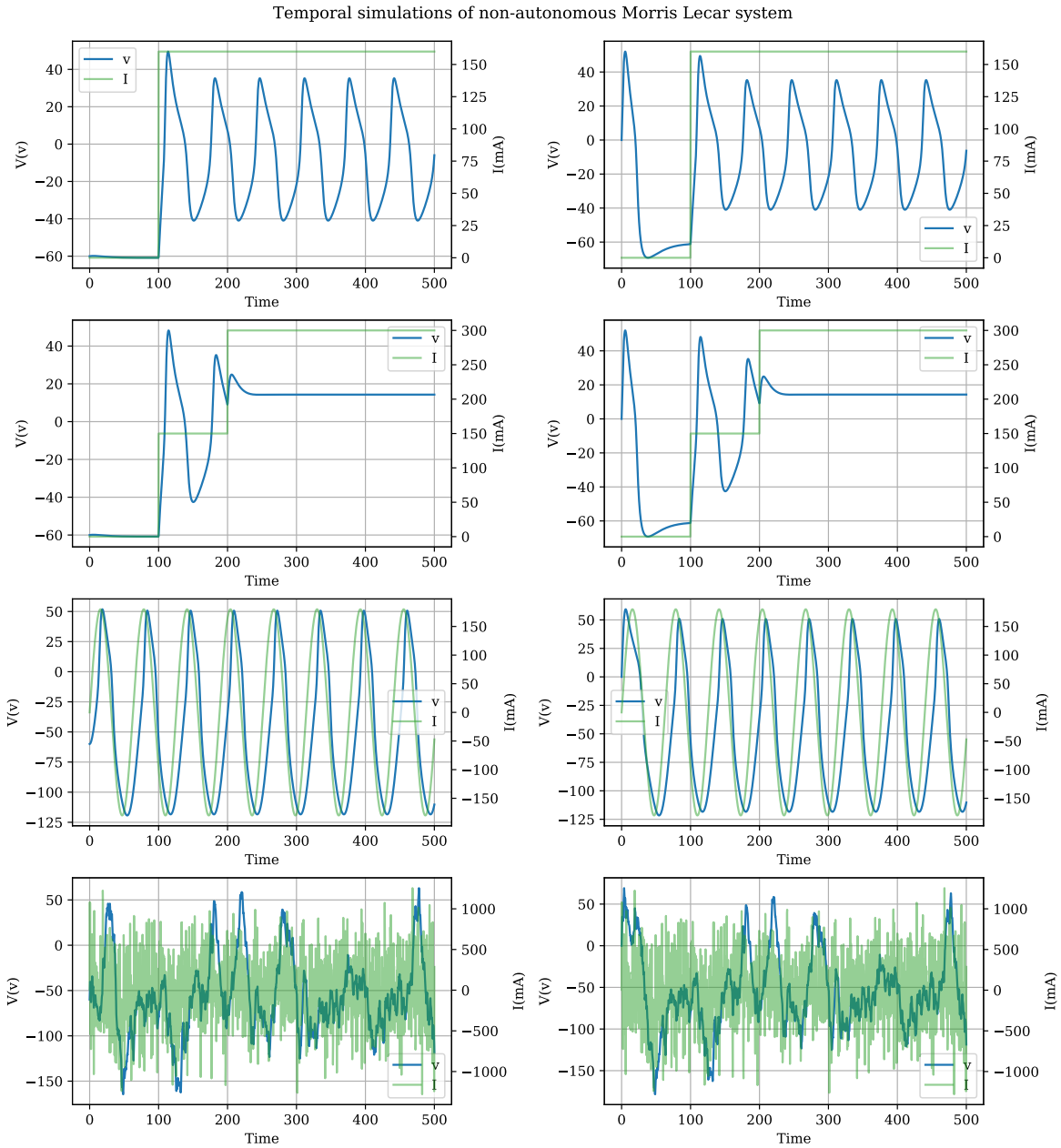

Figure 6: Non-autonomous system temporal simulations

The behaviour of the first three I_{app} functions is expected, but the fourth one is interesting. A noisy integrated signal (brownian movement) is capable of getting the system out of equilibria and creating spikes, while also creating a noisy voltage. In the next section we will further study stochasticity applied to this system.

Stochastic diferential equation (SDE)

So far we have seen continuous-time, continuous-state determinsitic systems in the form of Ordinary Differential Equations (ODE). Their stochastic counterpart are Stochastic Differential Equations (SDE).
Consider the now familiar non-autonomous ODE:

$$\frac{dy}{dt} = f(y,t)$$

The corresponding integral equation is:

$$y(t) = y(0) + \int_0^t f(y(s),s)ds$$

The SDE would be:

$$Y_t = f(Y_t,t)dt + g(Y_t,t)dB_t$$

Now Y_t is a random variable. B_t is the standard Brownian motion. The corresponding integral equation is:

$$y(t) = y(0) + \int_0^t f(Y_s,s)ds + \int_0^t g(Y_s,s)dB_s$$

As indicated in the statement, the Euler-Maruyama integration scheme will be used. In the next plot we see some time simulations of the SDE with different Intensities and initial conditions.

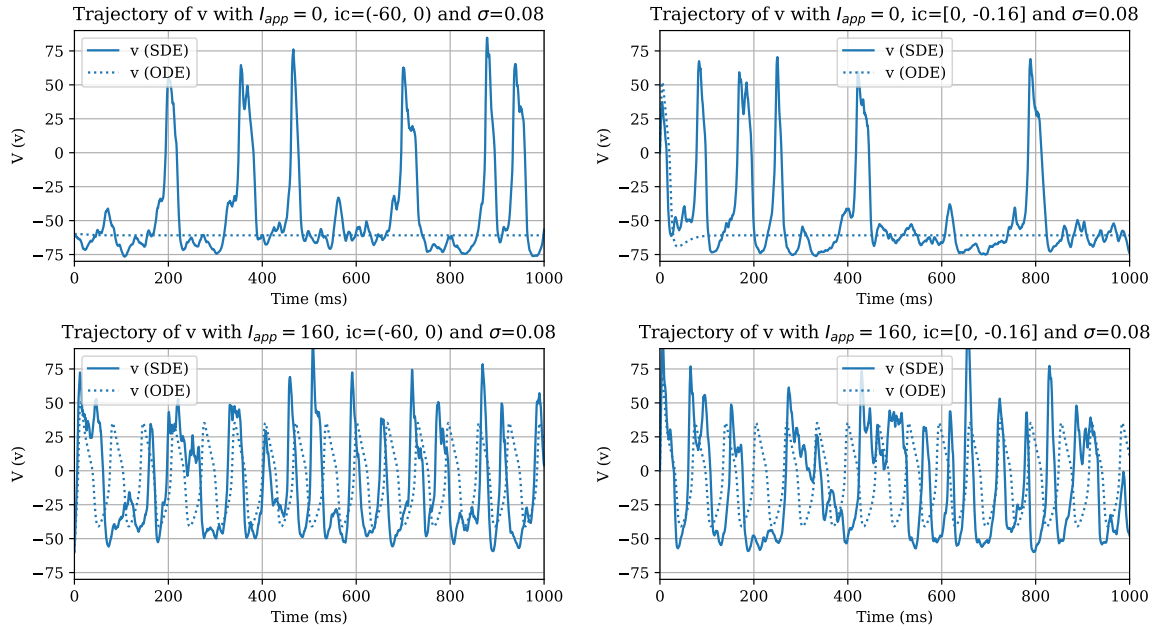

Figure 7: SDE time simulation

We can see how in the case with I_{app}=0 it produces many spikes during the 1000 ms simulations. In the case with I_{app}=160 the ODE system would be producing periodic oscillations, but now it completely loses the periodicity and produces them with random intervals.

In the phase diagram it is very noticeable the stochastic behaviour of the system and how it 'follows' the isoclines when kicked out of stability in the case with I_{app}=0. Also in the first plot we see how there are fewer lines in the right section as there aren't that many spikes in that case.

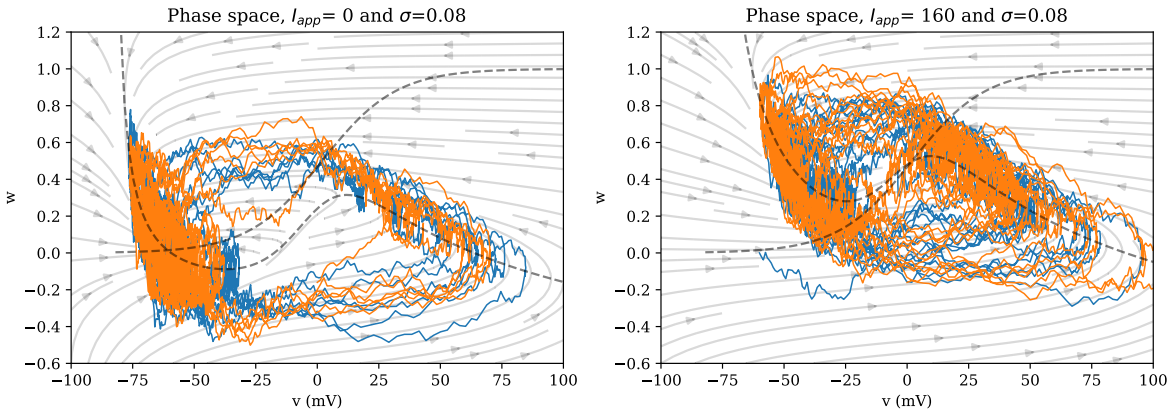

Figure 8: SDE phase diagram with σ=0.08

6.a Take a value of I_{app} in the subtreshold region and obtain 100 realizations of $v(t)$ for $t \in [0, 100]$. Compute the average and the standard deviation for every point of the trajectory and plot the results.

In this case instead of taking 100 realizations I have taken 500 realizations as now the histograms look better, with 100 realizations they were biased to one side or the other due to a low number of samples.

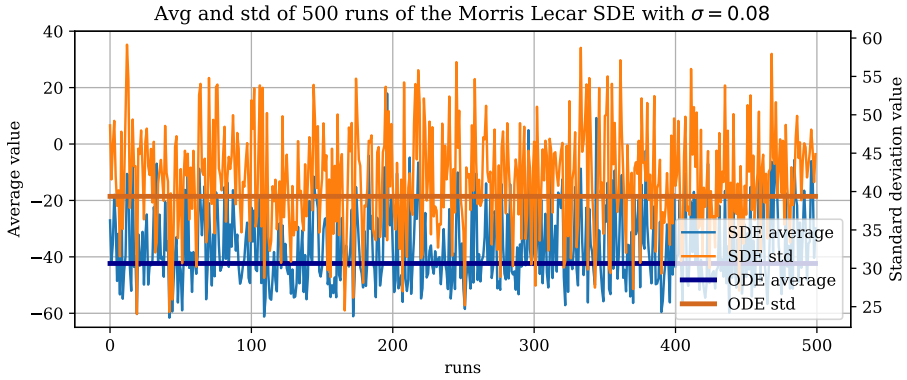

Figure 9: Average and STD of the Morris Lecar SDE

In my opinion it is easier to visualize in an histogram:

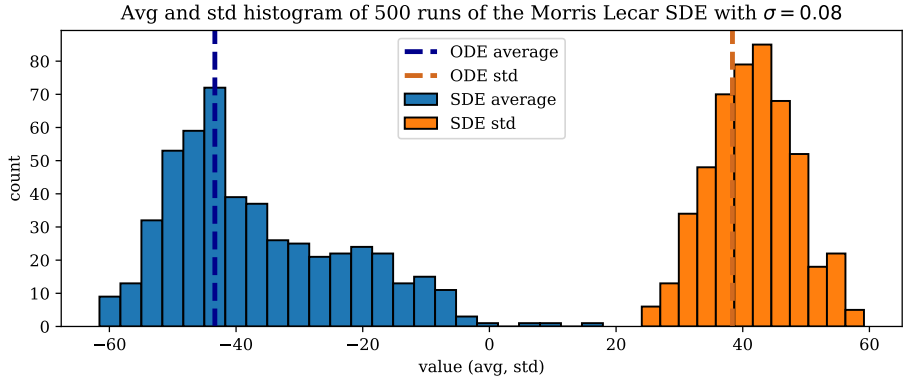

Figure 10: Average and STD of the Morris Lecar SDE

We can see how the mean and the standard deviation averaged out over a big number of observations converge towards the same value as the ODE mean and standard deviation. It is

beyond the goals of the project, but it is interesting to observe the skewness of the distribution. Also, the std is not completely symmetric. This makes us think about the "job" of the neuron as a filter since we put a gaussianly distributed input and we get a very different distribution.

6.b Plot the $f - I$ curve in terms of I_{app} for $\sigma \in \{0.1j\}_{j=1}^{20}$. What do you observe? Explain the differences with respect to σ

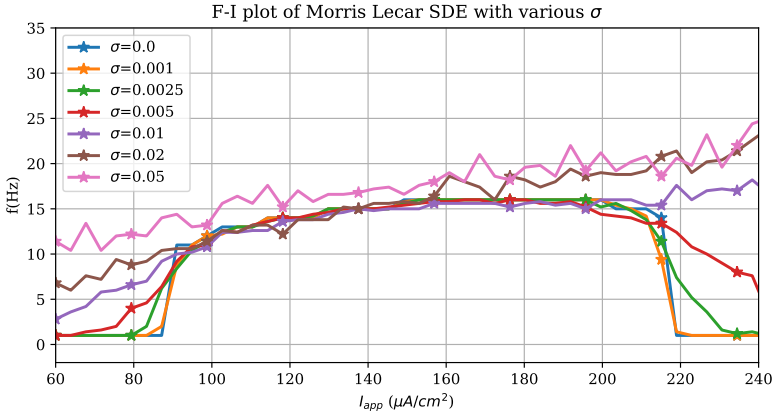

Figure 11: F-I curve with various σ, average of 5 simulations of 10^4ms

In this plot we observe the relationship between the intensities (I_{app}) and the frequency of the oscillations. There higher the variance of the SDE the flatter the F-I curve is, in the case with zero or low variances the F-I follows a "step function" between 85 and 220 aproximately. But with higher variances this "step function" becomes softer and eventually disappears with the higher variances.

As the neuron usually operates in the range near the first Hopf bifurcation (around 85 $\mu A/cm^2$ in our neuron) we can see how there are oscillations before the Hopf bifurcation. The neuron spikes because of the stochastic behaviour.

A comment about implementations

All the plots from this document have been produced by the author. They have been created by running numerical simulations with XPPAUTO, exporting the data to a file and plotting it using Python and the Matplotlib library, or have been simulated directly in Python and plotted using the same library. All the code for the visualizations is available in the form of jupyter notebooks in the following public git repository: `https://github.com/jaumecolomhernandez/mmb-mathneuroscience`

References

[1] C. Morris and H. Lecar, "Voltage oscillations in the barnacle giant muscle fiber," *Biophysics*, vol. 35, pp. 193–213, 1981.

[2] D. Culbert, "Giant barnacle photography." `https://eol.org/pages/4303198`, June 2011.

[3] A. L. Hodgkin and A. F. Huxley, "A quantitative description of membrane current and its application to conduction and excitation in nerve," *Physiology*, vol. 115, pp. 500–544, 1952.